



HAL
open science

Birth and growth of cavitation bubbles within water under tension confined in a simple synthetic tree

Olivier Vincent, Philippe Marmottant, Pedro A. Quinto-Su, Claus-Dieter Ohl

► **To cite this version:**

Olivier Vincent, Philippe Marmottant, Pedro A. Quinto-Su, Claus-Dieter Ohl. Birth and growth of cavitation bubbles within water under tension confined in a simple synthetic tree. *Physical Review Letters*, 2012, 108, pp.184502. <10.1103/PhysRevLett.108.184502>. <hal-00752084>

HAL Id: hal-00752084

<https://hal.science/hal-00752084v1>

Submitted on 14 May 2020

HAL is a multi-disciplinary open access archive for the deposit and dissemination of scientific research documents, whether they are published or not. The documents may come from teaching and research institutions in France or abroad, or from public or private research centers.

L'archive ouverte pluridisciplinaire HAL, est destinée au dépôt et à la diffusion de documents scientifiques de niveau recherche, publiés ou non, émanant des établissements d'enseignement et de recherche français ou étrangers, des laboratoires publics ou privés.



HAL Authorization

Birth and Growth of Cavitation Bubbles within Water under Tension Confined in a Simple Synthetic Tree

Olivier Vincent and Philippe Marmottant*

CNRS and Université de Grenoble, UMR 5588, Laboratoire Interdisciplinaire de Physique,
Grenoble, F-38041, France

Pedro A. Quinto-Su[†] and Claus-Dieter Ohl

Division of Physics and Applied Physics, School of Physical and Mathematical Sciences,
Nanyang Technological University, Singapore 637371, Singapore

(Received 21 June 2011; revised manuscript received 13 December 2011; published 3 May 2012)

Water under tension, as can be found in several systems including tree vessels, is metastable. Cavitation can spontaneously occur, nucleating a bubble. We investigate the dynamics of spontaneous or triggered cavitation inside water filled microcavities of a hydrogel. Results show that a stable bubble is created in only a microsecond time scale, after transient oscillations. Then, a diffusion driven expansion leads to filling of the cavity. Analysis reveals that the nucleation of a bubble releases a tension of several tens of MPa, and a simple model captures the different time scales of the expansion process.

DOI: 10.1103/PhysRevLett.108.184502

PACS numbers: 47.55.dd, 64.60.Q-

The dynamics of cavitation is a well-studied process in free liquids (cavitation in the wake of propellers, for instance), while cavitation in a microscopic confinement only recently received more attention. One important area of research is the transport of sap in trees and the potential blockage of this transport due to cavitation: These events can stop circulation of water in the vessels of real trees [1,2] or in synthetic ones that are used for microfluidic flow transport driven by evaporation [3–5].

The stability of water at negative pressure, i.e., under tension (see [6] for a review), can be tested with hydrogels where the tension is fixed through the relative humidity of the surrounding medium [3,7]. However, such a method features only the final equilibrium state and does not reveal anything about the cavitation process itself. The dynamics of cavitation involves fast time scales that are not known, apart from the fact that they are suspected to generate vibrations (noises in trees [8]).

In this study, we resolve the dynamics of cavitation of water inside hydrogel cavities. Cavitation can occur spontaneously or be triggered by a disturbance created by a laser pulse. The dynamics of the nucleated bubble and hydrogel cavity are recorded with a high-speed camera or a photodiode.

We use polyhydroxyethylmethacrylate (pHEMA) hydrogels of the same chemical composition as in Refs. [3,7], but with a periodic array of holes or cavities, created by using the novel experimental setup shown in Fig. 1(a). A Nd:YAG laser ($\lambda = 532$ nm, $t_p = 6$ ns) is coupled to an inverted microscope. The laser pulses are focused by a 40 \times water immersion microscope objective inside a thin layer of partially polymerized hydrogel that has been precured with UV light (dimensions $\sim 1.5 \times 1.5$ cm \times 0.7 mm). The hydrogel sample is bounded by

two microscope cover slides separated by polydimethylsiloxane spacers. A single cavity is created after a laser-induced optical breakdown inside the hydrogel sample. The system is coupled to an automated translation stage that allows the design of a regular array of holes. The shape of the cavities strongly depends on the degree of polymerization of the hydrogel: While they are smooth and spherical for low prepolymerization, they tend to form “cauliflower” shapes when more cured [Figs. 1(b) and 1(c)], in a manner very similar to what is observed when forcing air in a polyacrylamide gel [9]. Finally, the hydrogel is fully polymerized [Fig. 1(b)]. To fill the cavities with water, the hydrogel is boiled with water for a few days and soaked in degassed deionized water.

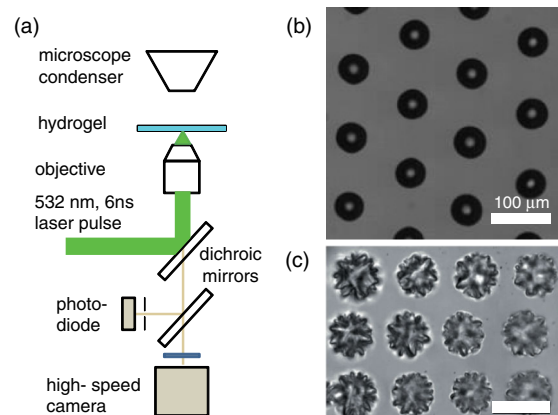


FIG. 1 (color online). (a) Experimental setup. (b) Microcavities in the hydrogel created by laser pulses with low UV precuring. (c) Microcavities when the hydrogel is precured for a longer time.

As the hydrogel samples are dried, water is set under tension because of evaporation. Cavitation spontaneously occurs when tension is strong enough or can be directly triggered with laser pulses, focused in the hydrogel, in the vicinity of water filled voids. The gel is sometimes slightly altered [apparition of a gray spot, Fig. 2(a)]. We speculate that a mild pressure wave is created, travels over the microcavity, and thereby increases the liquid tension for a brief moment. This mechanical disturbance in the hydrogel is able to trigger cavitation in neighboring microcavities, if under tension. The dynamics of cavitation is recorded with a high-speed camera at frame rates of up to 432 000 frames per second, with an exposure time of $1 \mu\text{s}$. In addition, the central part of the image can be projected simultaneously onto a photodiode with a rise time of $0.03 \mu\text{s}$ and bandwidth of 12 MHz, providing a measurement of the mean intensity in order to access faster dynamics.

Fast time scales.—Our recordings reveal that a single bubble is nucleated and that its volume quickly reaches a finite value, within 1 or 2 μs [Figs. 2(a)–2(c)]. We captured the first image of the nucleated bubble after a delay of 1 μs after arrival of the laser pulse. If these images are motion blurred due to the exposure time of $1 \mu\text{s}$, they show a

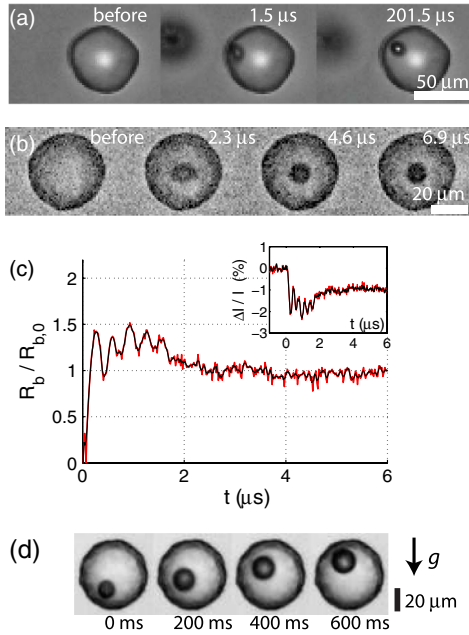


FIG. 2 (color online). Image sequences showing the birth of a cavitation bubble (a) triggered by a laser pulse aimed away from microcavity, here on the left (b) spontaneous without triggering, here under $40\times$ objective. (c) Photodiode recording on a cavity with a radius of $40 \mu\text{m}$: estimated apparent bubble radius as a function of time, normalized by the bubble radius just after nucleation, for a single experiment. Red, experimental data; black, slightly filtered signal. Inset: Recorded relative variations of the photodiode signal from which the radius is estimated. (d) Long term rise of a bubble in a vertical sample.

transient nonspherical shape; see the second image in Fig. 2(b). On the photodiode signal [Fig. 2(c)], we record transient high-frequency oscillations of several megahertz, that we interpret as oscillations of the radius, with an initial velocity as high as 30 m/s . We assumed that the change in light intensity is proportional to the apparent bubble area on the images.

The following images of the high-speed recording show that the bubble after nucleation reaches a temporary equilibrium radius and then slowly grows. This is in contrast to cavitation nucleation in a free liquid, where the bubble expands to a maximum size and then rapidly collapses due to the pressure of the surrounding liquid. Experiments imaged from the side also evidence that bubbles rise due to their buoyancy [Fig. 2(d)], meaning they are not attached by a contact line and are quickly spherical.

The instantaneous volume of the bubble (V_b) and of the cavity (V_c) are obtained by extracting an effective radius from image analysis (Fig. 3), consisting in tracing isovalue lines on gray level bitmaps. Interestingly, the volume of liquid $V_l = V_c - V_{b,0}$ just after nucleation decreases. This is due to the compressibility of water, which has an adiabatic bulk modulus [10] $K_l = 2.2 \text{ GPa}$ at 20°C . Therefore, the variation of liquid volume $\Delta V_l (= \Delta V_c - V_{b,0})$ gives information on the pressure change Δp in the liquid:

$$\Delta p = K_l \frac{\Delta V_l}{V_l}. \quad (1)$$

We performed this analysis for a total of 17 bubbles (see Fig. 3), showing that the released pressure amounts to values ranging within the tens of MPa range ($30 \pm 16 \text{ MPa}$). Because of the measurement error in the image analysis, the estimated pressure presents a lot of

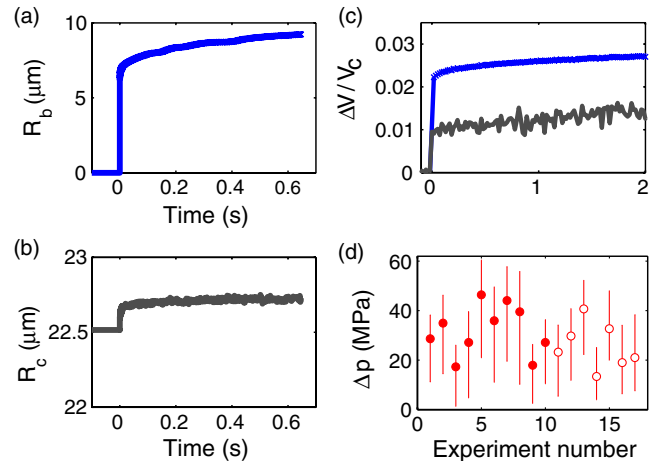


FIG. 3 (color online). Evolution of (a) the bubble radius R_b and (b) the cavity radius R_c . (c) We infer that the bubble volume increase is larger than cavity volume increase, meaning that the liquid volume decreases. (d) Estimation of the tension that is relaxed, for triggered (full circles) and spontaneous bubbles (open circles).

uncertainty but is comparable to that measured for cavitation in static hydrogels with the same composition (22 MPa) [3,7] and to other experimental methods [6]. Note that the pressure released by triggered cavitation is of the same order as with spontaneous cavitation [Fig. 3(d)]. Indeed, the laser perturbation is not very large, and in order to trigger cavitation we had to wait for the pressure to be close to the spontaneous threshold, i.e., when cavitation occurs spontaneously on nearby cavities.

From this pressure, the stored elastic energy of water can be evaluated to be $E_p = -\frac{1}{2}\Delta p V_b$. If all this energy was released into kinetic energy, writing $E_k = \frac{3}{2}\rho_l V_b \dot{R}_b^2$ for a bubble in liquid [11] of density ρ_l , we could expect bubble oscillations with maximum velocity $\dot{R}_b = (-\Delta p/3\rho_l)^{1/2} \sim 100$ m/s and a characteristic time $\tau = R_b/\dot{R}_b$ of $0.1 \mu\text{s}$ only (for a cavity such that $R_b = 10 \mu\text{m}$, $R_c = 40 \mu\text{m}$). This time is of the same order as the observed initial relaxation time of the light intensity signal ($0.3 \mu\text{s}$). The system shows oscillations that are rapidly damped, probably because of dissipation in the gel surrounding the microcavities, besides viscous dissipation in water or acoustic emissions.

One may wonder about the content of the cavitation bubble. After cavitation, the bubble quickly fills with water vapor, which has a diffusion coefficient $D_{\text{vap}} = 2.4 \times 10^{-5} \text{ m}^2 \text{ s}^{-1}$. With R_0 the initial size of the bubble, the typical vapor filling time is $R_0^2/D_{\text{vap}} \sim 10^{-5} \text{ s}$, thus longer than the initial dynamics. Then it also probably fills with air that was dissolved in water and in the hydrogel. These processes might slightly change the pressure inside the bubble but cannot account for the continuous post-nucleation expansion of the cavitation bubble.

Long time scales.—Indeed, after its fast expansion to the volume $V_{b,0}$, the bubble is not static but slowly grows, until it completely fills the cavity, after a time of approximately 100 s. To quantify this growth, we analyzed the evolution of the volumes of the cavity and of the bubble (Fig. 4). The bubble expansion $V_b - V_{b,0}$ versus time follows a power law over more than 5 decades of time, with exponents in the range 0.35–0.45 [Fig. 4(c)].

Neglecting evaporation, there are only two ways to make the bubble grow: increase the volume of the cavity or transfer liquid from the cavity to the gel. The analysis of $V_c(t)$ shows that the size of the cavity indeed increases with time [Fig. 3(c)]. However, since the bubble eventually fills the whole cavity, an outwards flow of water must occur.

We developed a simple model to account for the power-law expansion of the cavitation bubble. In the following, we will describe only the growth of the bubble by flow in the gel and hypothesize a constant cavity volume.

When cavitation occurs, the pressure in the liquid suddenly relaxes from a homogeneous negative value $p_l = -\Delta p$ to a local value $p_l = p_g - 2\sigma/R_0$, with $2\sigma/R_0$ the capillary pressure due to water surface tension and p_g the gas pressure inside the bubble. We then have

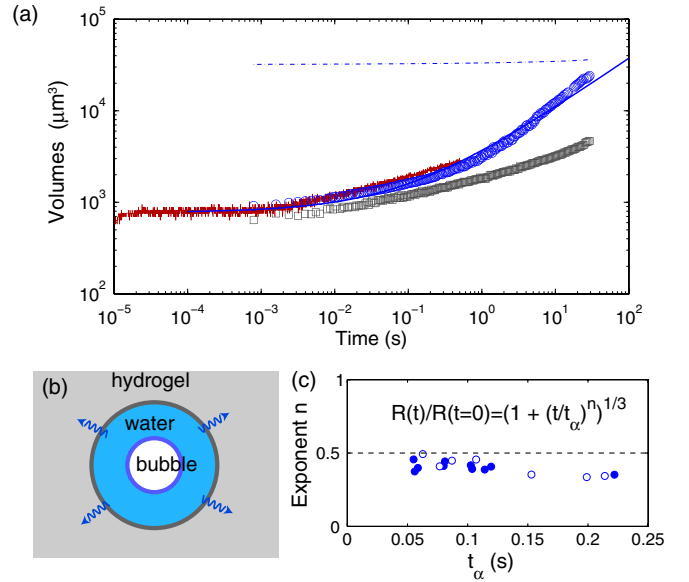


FIG. 4 (color online). (a) Long time growth of the bubble volume (red line, photodiode signal after oscillations; blue circles, camera) and of the cavity (V_c , dashes; ΔV_c , gray open squares). The bubble volume V_b is fitted with Eq. (3) (continuous blue line). (b) Diagram showing the origin of the growth: diffusion of water in the hydrogel. (c) Growth exponent for the bubble size for triggered (full circles) and spontaneous bubbles (open circles).

$|p_l| \ll \Delta p$. This locally changes the osmotic pressure $\Pi = P - p_l$ in the gel near the surface of the cavity, where P is the external isotropic stress (here being constant, equal to atmospheric pressure). Incidentally, a gradient of osmotic pressure $\nabla \Pi$ develops across the gel, entailing water fluxes \mathbf{q} which follow Darcy's law $\mathbf{q} = -\frac{k(\phi)}{\mu} \nabla p_l = \frac{k(\phi)}{\mu} \nabla \Pi$, with k the permeability, μ the viscosity, and ϕ the polymer volume fraction.

The conservation of mass implies $\frac{\partial \phi}{\partial t} = \phi \nabla \cdot \mathbf{q}$ [12]. A change in volume fraction results in a change in osmotic pressure, and the last equation can be rewritten as

$$\frac{\partial \Pi}{\partial t} = K_{\text{sw}} \nabla \cdot \left(\frac{k}{\mu} \nabla \Pi \right) \simeq D \nabla^2 \Pi, \quad (2)$$

where $K_{\text{sw}} = \phi \frac{\partial \Pi}{\partial \phi}$ is the swelling modulus of the gel, describing how the polymer network of the gel swells or shrinks in response to water pressure changes [13]. Equation (2) is similar to the one developed for the sedimentation of a colloidal solution [14]. Assuming low variations of permeability, we have approximated the right-hand side by $D \nabla^2 \Pi$. The water content and osmotic pressure therefore follow a diffusion equation, with a diffusion coefficient $D = K_{\text{sw}} k / \mu$. The value of this coefficient is around $D \sim 10^{-11} \text{ m}^2 \text{ s}^{-1}$ [15].

The diffusion of pressure entails fluxes that follow $q = k/\mu \times \Delta p / \sqrt{\pi D t}$, over the cavity surface $S = 4\pi R_c^2$. The

transferred volume is therefore $dv_l/dt = qS$, so that, under the hypothesis of a constant cavity volume V_c , the bubble volume departs at long time scales from the initial volume V_0 [given by Eq. (1)] along

$$\frac{V_b}{V_0} = 1 + \left(\frac{t}{t_\alpha}\right)^n \quad (3)$$

with $n = 1/2$ and $t_\alpha = \pi \frac{R_c^2}{D} \left(\frac{K_{sw}}{6\Delta p} \frac{V_0}{V_c}\right)^2$, which represents the time for which the bubble volume has doubled.

Fitting the experimental curves of bubble growth of Fig. 4(a) (for times $t < 1$ s) provides t_α and exponent n values displayed in Fig. 4(c). The value of n is close to the predicted value $1/2$, except for the largest characteristic time t_α . The observed range of t_α is also in excellent agreement with the expected value, predicted by using the negative pressure measured in the first section: With $\Delta p = 20$ MPa, $K_{sw} = 100$ MPa, $D = 10^{-11}$ m² s⁻¹, and values extracted from one experiment of $R_c = 23$ μ m and $R_0 = 6.8$ μ m, one finds $t_\alpha = 0.08$ s. The final filling of the bubble when $R_b = R_c$ can be deduced from Eq. (3) and occurs at a time

$$t_f = \pi \frac{R_c^2}{D} \left(\frac{K_{sw}}{6\Delta p}\right)^2, \quad (4)$$

where we have neglected V_0 in front of V_c . Using the same numerical values as above, one finds $t_f = 115$ s, in very good agreement with the experimental observations. Note that the cavity volume is not constant in the experiment, so that the diffusion model should describe primarily the transferred liquid volume. Preliminary analysis of this volume provides larger growth exponents: This phenomenon is still under investigation. Also, another challenge is to understand why, surprisingly, the curves of Fig. 4(a) show that there is no detectable transfer of fluid to the gel during the first 10 ms after cavitation, since $V_b(t)$ and $\Delta V_c(t)$ initially differ by a constant offset. Then, an outward flow proceeds, which results in gas filling of the cavity.

In conclusion, we report in this Letter the first direct observations of spontaneous and triggered cavitation of water under static tension in confined geometries. The nucleated bubble initially expands at a submicrosecond time scale, driven by a tension of tens of MPa. These extreme tensions lead to uncommon facts in microfluidics: very fast velocities (30 m/s) and visible liquid volume changes associated with inertia, as can be seen on the initial damped oscillations of the bubble. Work is under way to fully characterize these oscillations. Also, the cavitation events studied here show milder dynamics as compared to a free liquid with successive collapses. Thus, cavitation in water under tension leads to nucleation of bubbles but not to the destructive effects observed during cavitation bubble collapse. The presence of hydrogel in trees has been demonstrated recently [18] and could thus have a role in the prevention of damage by cavitation events.

We also investigated the following slow growth of the bubble, which is limited by liquid flow in the surrounding gel, rehydrating it. Besides being useful for the design of hydrogel-made microfluidic devices, this fact leads to two remarks.

First, diffusion in a hydrogel is a complex process: The coefficient D arises from a subtle balance between the elasticity and the permeability of the gel [Eq. (2)], which change when it dries or hydrates. Since the hydrogel becomes softer as it rewets, this might slow the diffusion process as the cavitation bubble expands, explaining the fact that the growth exponents seen in Fig. 4 are always lower than expected from normal diffusion. Another challenge is to explain the origin of the latency time of about 10 ms after cavitation when no flow towards the gel occurs.

Second, the release of tension propagates in the gel when it is rewetted by water, and this effect should be felt in close-by cavities. Indeed, when focusing the laser in the middle of three cavities at the same distance from each one, we noticed that the last triggered cavitation required much more laser energy than the first one. This interaction might stabilize neighboring cavities, but only for limited times, since diffusion eventually smooths out the temporary pressure peak. Such a phenomenon suggests that cavitation propagation can be hindered by negative correlations. Applied to the context of sap transport, we hypothesize that this phenomenon may play a role in trees to regulate tension in the xylem.

The authors thank Dr. Roberto Gonzalez and Dr. Keita Ando for discussions and help with the experiments and the French-Singapore Merlion Grant No. 2.08.09 for financial support.

*philippe.marmottant@ujf-grenoble.fr

†Present address: ICN-UNAM, C.P. 04510, México, D.F., México.

- [1] M. T. Tyree, *Nature (London)* **423**, 923 (2003).
- [2] H. Cochard, *C.R. Physique* **7**, 1018 (2006).
- [3] T. D. Wheeler and A. D. Stroock, *Nature (London)* **455**, 208 (2008).
- [4] X. Noblin, L. Mahadevan, I. A. Coomaswamy, D. A. Weitz, N. M. Holbrook, and M. A. Zwieniecki, *Proc. Natl. Acad. Sci. U.S.A.* **105**, 9140 (2008).
- [5] P. Moreau, J. Dehmoune, J.-B. Salmon, and J. Leng, *Appl. Phys. Lett.* **95**, 033108 (2009).
- [6] E. Herbert, S. Balibar, and F. Caupin, *Phys. Rev. E* **74**, 041603 (2006).
- [7] T. D. Wheeler and A. D. Stroock, *Langmuir* **25**, 7609 (2009).
- [8] M. T. Tyree and M. A. Dixon, *Plant Physiol.* **72**, 1094 (1983).
- [9] S. Kundu and A. J. Crosby, *Soft Matter* **5**, 3963 (2009).
- [10] At 20 °C, the adiabatic and isothermal compressibilities of water are very close and differ by less than 1%. Their variation with pressure is also small: about 2.5% for each 10 MPa.
- [11] T. G. Leighton, *The Acoustic Bubble* (Academic, London, 1994).

- [12] Conservation of mass for the polymer implies $\phi \delta V = \text{cst}$ for an *elementary* hydrogel volume δV . Its variation is thus $\frac{d\delta V}{dt} = -\frac{\delta V}{\phi} \frac{d\phi}{dt}$, while conservation of mass for the fluid implies $\frac{d\delta V}{dt} = \frac{d\delta V_f}{dt} = -\delta V \nabla \cdot \mathbf{q}$, which gives the formula in the text.
- [13] This swelling modulus under constant isotropic stress can also be expressed as $K_{\text{sw}} = V \frac{\partial p}{\partial V}$, V being the total hydrogel volume. It is equivalent to a compression bulk modulus, but with opposite sign, as a polymer network inflates when increasing the solvent pressure.
- [14] C. Kim, Y. Liu, A. Kühnle, S. Hess, S. Viereck, T. Danner, L. Mahadevan, and D.A. Weitz, *Phys. Rev. Lett.* **99**, 028303 (2007).
- [15] This value is deduced from measurements of the relaxation time of a drying hydrogel. For our pHEMA hydrogel, we estimate $K_{\text{sw}} \approx 100$ MPa from Flory's theory [16], so the estimated hydrogel permeability is very low: $k/\mu = 10^{-19}$ m²/Pa s. For comparison, with polyacrylamide hydrogel, Tanaka, Hocker, and Benedek [17] find $D \sim 4 \times 10^{-12}$ m² s⁻¹. This diffusion coefficient is similar to the present pHEMA hydrogel but originates from very different values of elasticity and permeability, since they have $k/\mu = 1/f = 5 \times 10^{-15}$ m²/Pa s but a much softer gel.
- [16] P.J. Flory, *Principles of Polymer Chemistry* (Cornell University, Ithaca, NY, 1955).
- [17] T. Tanaka, L.O. Hocker, and G.B. Benedek, *J. Chem. Phys.* **59**, 5151 (1973).
- [18] M.A. Zwieniecki, P.J. Melcher, and N. Michele Holbrook, *Science* **291**, 1059 (2001).